Rotational Barrier in Ethane (1)

The Case for Steric Repulsion Causing the Staggered Conformation of Ethane

*F. Matthias Bickelhaupt and Evert Jan Baerends**

It has recently been argued[1,2] that the barrier to rotation around the C–C bond in ethane is not to be explained by the generally accepted picture of steric hindrance between vicinal C–H bonds in the eclipsed conformation but is caused by more favorable orbital interaction in the staggered conformation. In that conformation the C–H bonds at opposite ends of the molecule have an in-plane *trans* conformation which is favorable for interaction of the σ* antibonding orbital of one C–H unit with the occupied σ_{C-H} bonding orbital at the other side (six such pairs). This view has been advocated with

[*] Prof. E. J. Baerends, Dr. F. M. Bickelhaupt
Afdeling Theoretische Chemie
Faculty of Science, Vrije Universiteit
Scheikundig Laboratorium, De Boelelaan 1083
1081 HV Amsterdam (The Netherlands)
Fax: (+31) 20-444-7629
E-mail: baerends@chem.vu.nl

 DOI: 10.1002/ange.200350947

natural bond orbital (NBO) analyses for a long time by Weinhold and co-workers.[3–6] Pophristic and Goodman[1] deleted the σ–σ* NBO interactions and found that the ethane preferred structure reverts to eclipsed, thus providing substantiation of the orbital-interaction view within the NBO framework.

The issue is interesting and important[7–9] but also controversial. We have reinvestigated the rotation around the C–C bond in ethane employing a widely used and straightforward electronic-structure analysis method (see below). It turns out that it is very important to take carefully into account the effect of geometry changes during rotation around the C–C bond, notably the C–C bond stretching when going towards the eclipsed conformation, as indeed already stressed by England and Gordon[14] and Goodman and co-workers.[15] We will see that the interpretation of the barrier as caused by steric repulsion between vicinal C–H bonds is fully corroborated by this analysis, and we conclude it is perfectly valid for organic chemists to adhere to this view. We comment on the possible source of the difference between our analysis and the NBO one.

Our electronic-structure analysis of the eclipsed versus staggered conformations uses a few well-defined terms, which can be used with exact wavefunctions of the interacting fragments, or with approximate wavefunctions. We start the formation of the C–C bond between two methyl fragments by employing the wavefunctions Ψ^A and Ψ^B of the isolated fragments to build a "zeroth-order" wavefunction Ψ^0 in which only the Pauli exclusion principle is enforced by antisymmetrization ($\hat{A}$) and renormalization (N) of the product function $\Psi^A\Psi^B$: $\Psi^0 = N\hat{A}[\Psi^A\Psi^B]$. In our case we use a determinantal wavefunction with the (overlapping) Kohn–Sham orbitals of the fragments. The antisymmetrization, which is usually performed after orthogonalization of the fragment orbitals, which does not change the wavefunction, see ref. [19], leads to a density ρ^0 which differs from the superposition $\rho^A + \rho^B$. One usually separates the electrostatic interaction (ΔV_{elstat}) between the (unmodified, interpenetrating) electronic charge cloud (ρ^A) and nuclei of one fragment with those of the other (ρ^B) from the total ΔE^0, defining the Pauli repulsion ΔE_{Pauli} as in Equation (1).

$$\Delta E^0 = E[\Psi^0] - E[\Psi^A] - E[\Psi^B] = \Delta E_{Pauli} + \Delta V_{elstat} \quad (1)$$

ΔE^0 is repulsive owing to the strongly repulsive ΔE_{Pauli} term. The repulsion is caused by an increase in the kinetic energy, which is an effect of the antisymmetrization (usually calculated by orthogonalization) among the occupied orbitals ("orthogonality tails"). This outweighs a generally more negative potential energy, see ref. [19] for detailed discussion of the various energy contributions. The energy lowering as a result of the formation of the electron-pair bond is not contained in ΔE^0. This energy, and in addition the occupied-virtual-orbital interactions which account for the polarization of the methyl fragments and for the possible vicinal charge-donation type of interaction from a σ_{C-H} orbital on fragment A to a σ^*_{C-H} orbital on fragment B, are included in the relaxation or orbital-interaction step with energy contribution ΔE_{oi} which describes the energy relaxation from $E[\Psi^0]$ to the final energy $E[\Psi^{AB}]$ of the wavefunction Ψ^{AB} of the ethane molecule. The total bond energy ΔE will be given by Equation (2).

$$\Delta E = \Delta E_{Pauli} + \Delta V_{elstat} + \Delta E_{oi} \quad (2)$$

The relaxation energy $\Delta E_{oi} = E[\Psi^{AB}] - E[\Psi^0]$ is defined for exact wavefunctions but also for the Hartree–Fock model and for Kohn–Sham DFT. Since we use these orbital models we refer to it as the orbital-interaction term ΔE_{oi}. These same terms are also used in the scheme originally introduced by Morokuma and co-workers[10–13] at the Hartree–Fock level, but we do not apply Morokuma's further break-down of the ΔE_{oi} term in the basis-set-dependent charge-transfer and polarization (and mix) terms. The same scheme, but with a different partitioning (symmetry based) of the ΔE_{oi} term, was used by Ziegler and co-workers[16–19] in a DFT context, which has the advantage of providing us with rather accurate energetics. We use an extension to open-shell systems where an electron-pair bond is formed.[20]

We stress that this energy decomposition, apart from being well established and widely practiced, is also general in the sense that the terms are defined also for high-quality (fully correlated) fragment and total wavefunctions. The definition of Pauli repulsion (or exchange repulsion) used here is generally used, for example, in the theory of intermolecular forces.

The total barrier height going from staggered to eclipsed ethane is calculated with the Becke 88–Perdew 86 functional of DFT to be 2.54 kcal mol^{-1}, with full optimization of C–C bond lengths and CH_3 geometry in both conformations. This situation compares reasonably with the experimental value of 2.875 kcal mol^{-1}.[21] Basis-set superposition errors (BSSE) are very small for the large STO basis sets we are using, and totally insignificant for the barrier height (correction for BSSE changes the barrier by 0.04 kcal mol^{-1}). To analyze the origin of the barrier we build ethane from two "prepared" methyl fragments. This preparation involves deforming the planar methyl radicals to exactly the optimized geometries they have in the two conformations. Although the difference in bending and C–H bond lengths for the two optimum CH_3 conformations (which we denote as CH_3(e) for eclipsed and CH_3(s) for staggered ethane, respectively) is quite small (0.5° larger ∢C-C-H angle, 0.001 Å shorter C–H bonds for eclipsed than staggered), the preparation energy for two CH_3(e) (19.32 kcal mol^{-1}) is 1.1 kcal mol^{-1} higher than for two CH_3(s) (18.24 kcal mol^{-1}). This difference is not insignificant compared to the barrier energy, and the effect of CH_3 deformation will be discussed later, but first we address the crucial role played by the C–C bond length. Figure 1 shows the behavior of the Pauli repulsion energy between the prepared methyl fragments as a function of the rotation angle φ. The ΔE_{Pauli} versus φ curves are given for both the optimum C–C separation for the staggered (upper curve) and the eclipsed (lower curve) conformations (the CH_3 geometries are also fixed at staggered and eclipsed values). At both separations the Pauli repulsion is a minimum for the staggered conformation, and goes to a maximum which is 2.35–2.60 kcal mol^{-1} higher at the eclipsed conformation. This

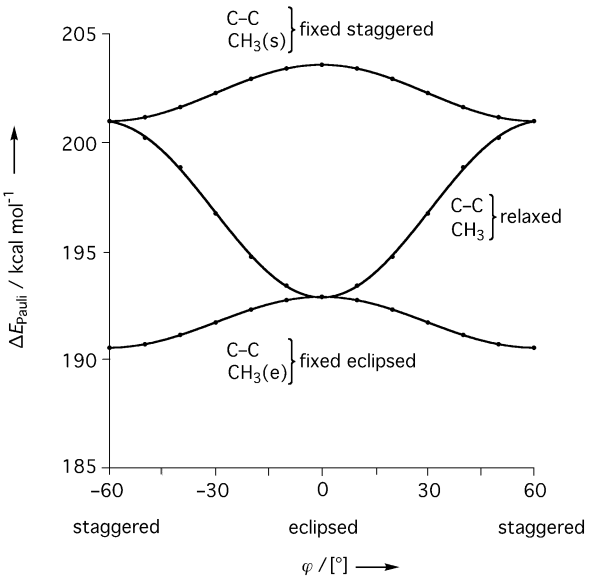

Figure 1. The Pauli repulsion energy between two CH_3 radicals as a function of the dihedral ∢HCCH angle φ. Upper curve: the C–C separation and the geometric parameters of the two CH_3 fragments are fixed to the values for staggered ethane (R_{eq}(staggered) and CH_3(s)). Lower curve: the C–C separation and geometric parameters of the two CH_3 fragments are fixed at the values for eclipsed ethane (R_{eq}(eclipsed) and CH_3(e)). Middle curve: the fully optimized geometry at each value of φ.

result would seem to indicate that Pauli repulsion is the origin of the barrier, as assumed in the standard view. However, we have to be careful with the strong effect of the C–C bond length on the Pauli repulsion. Even though the optimal C–C separations differ only a little (1.5315 Å for staggered and 1.5455 Å for eclipsed), it is to be noted that the energies of the Pauli repulsion at the longer bond length R_{eq}(eclipsed) are over the whole φ range some 10 kcal mol^{-1} lower than at the shorter bond length. In Figure 1 we also show the Pauli repulsion as a function of φ when we optimize the C–C bond length (and also the CH_3 geometries) at each φ value. Owing in particular to the C–C bond lengthening, the Pauli repulsion is lowest along this curve in the eclipsed conformation. However, it would not be logically correct to infer that steric repulsion favors the eclipsed conformation (and that therefore an alternative mechanism has to be invoked to explain the preference for the staggered conformation). Such a conclusion cannot be drawn from the behavior of ΔE_{Pauli} along a single path through the molecular configuration space (such as the middle curve of Figure 1). For instance, the lower curve shows that when the C–C separation is fixed at the longer bond length (R_{eq}(eclipsed)) of the eclipsed conformation, the Pauli repulsion would still favor rotation to the staggered conformation.

How, then, can we understand the behavior of the Pauli repulsion as a function of φ when all other geometry parameters are fully optimized (i.e. the middle curve in Figure 1)? Let us take staggered ethane at its optimum geometry and first rotate it with fixed R(C–C) and CH_3(s) geometry to the eclipsed conformation (upper curve), which leads to 2.60 kcal mol^{-1} more Pauli repulsion. The sum of ΔE_{oi} and ΔV_{elstat} adds only 0.07 kcal mol^{-1} to the barrier energy with these geometry constraints. When we keep the molecule in the eclipsed conformation but relax the other geometry parameters, the molecule responds by lowering the total energy slightly (the final barrier is 2.54 kcal mol^{-1}) by lengthening the C–C bond and bending back the CH_3 units. The individual energy components change much more, which is possible since their changes with C–C bond lengthening have opposite signs. The Pauli repulsion lowers by approximately 10 kcal mol^{-1}, in fact much more than the initial rise of only 2.6 kcal mol^{-1}. In Figure 2 we show the various terms—Pauli repulsion, electrostatic interaction, and orbital interaction—as a function of C–C separation, which is the most important

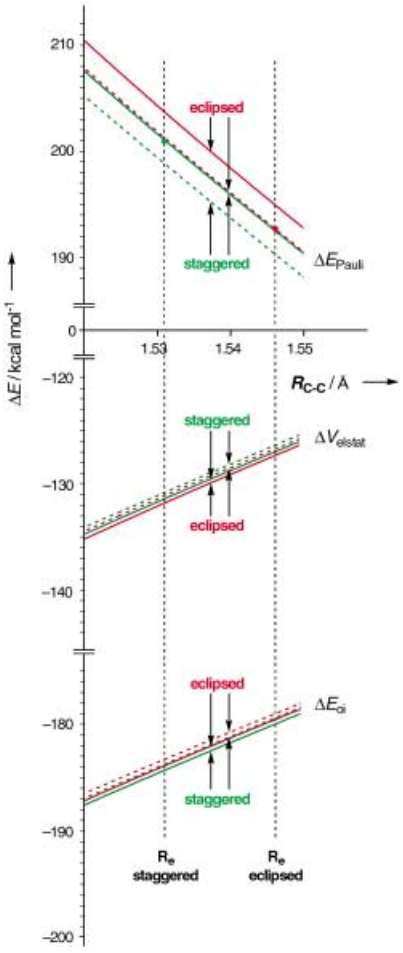

Figure 2. The three contributions ΔE_{Pauli}, ΔV_{elstat}, and ΔE_{oi} (see text) to the total bond energy between two CH_3 radicals, as a function of the C–C separation. The full lines are for CH_3(s) (optimized CH_3 geometry in staggered ethane); red for eclipsed conformation, green for staggered conformation. The broken lines are for CH_3(e) (optimized CH_3 geometry in eclipsed ethane); red for eclipsed conformation, green for staggered conformation. The Pauli repulsion in the equilibrium conformation of staggered ethane is denoted by a green dot, and the Pauli repulsion in the equilibrium conformation of eclipsed ethane by a red dot. Since accidentally the Pauli repulsion curves for staggered ethane with CH_3(s) (solid green line) and eclipsed ethane with CH_3(e) (broken red line) practically coincide, one has been shifted up and the other shifted down by 0.1 kcal mol^{-1} for clarity.

geometric parameter. To separate the effect of C–C bond-length change from the effect of CH_3 flexing we first focus on the curves for fixed CH_3(s) geometry (solid line, green for staggered ($\varphi = 60°$), red for eclipsed ($\varphi = 0°$)). At all distances shown the Pauli repulsion is strongest in the eclipsed case. The difference in Pauli repulsion between eclipsed and staggered ethane is considerably larger than the differences for the other energy terms, ΔV_{elstat} and ΔE_{oi}. A crucial observation is that also the increase of the Pauli repulsion with the shortening bond length is greater in the eclipsed case, that is, at the shorter distance R_{eq}(staggered) the gradient of the red line is larger than of the green line. The equilibrium bond length is not determined by the absolute values of the total energy or its components, but simply by the requirement that the derivative of the total energy with respect to the C–C bond length be zero. Since the other energy components (ΔE_{oi} and ΔV_{elstat}) are virtually parallel for eclipsed and staggered ethane, the larger gradient of the steric repulsion curve in the eclipsed case, at shorter bond length, such as R_{eq}(staggered), will drive the molecule in that conformation to a state with a longer equilibrium C–C bond length. This situation explains why R_{eq}(eclipsed) is longer, as indicated in Figure 2. The resulting steric repulsion in the eclipsed conformation at that long equilibrium bond length (red dot in Figure 2) is lower than in the staggered conformation at its shorter equilibrium bond length (green dot). This should not be mistaken as a contradiction of the intuitive notion that the eclipsed conformation suffers from stronger steric repulsion, which we see is true at any given C–C bond length.

When we now consider the effect of CH_3 flexing (broken lines for CH_3(e)), the picture remains essentially the same. The flexing of CH_3 towards CH_3(e) reduces the overlap between the orbitals of the vicinal C–H bond, hence it reduces the Pauli repulsion. So the ΔE_{Pauli} curves for CH_3(e) are lowered with respect to the curves for CH_3(s) (Figure 2). Starting again with rotation of fixed CH_3(s) at R_{eq}(staggered) from staggered to eclipsed (from green dot to solid red line), the Pauli repulsion does not only increase, but will also get a steeper gradient for CH_3 bending, as it did for C–C bond lengthening. So the Pauli repulsion and its gradient will become lower by bending CH_3 back to CH_3(e). Accidentally, going from CH_3(s) to CH_3(e) in the eclipsed conformation (from solid red line to broken red line) lowers the Pauli repulsion practically by the same amount as rotation of CH_3(s) from staggered to eclipsed conformation made it rise.

The optimized geometry (C–C separation and CH_3 bending) in the eclipsed conformation is solely determined by the zero gradient of the total energy with respect to the allowed nuclear displacements. This point, at R_{eq}(eclipsed) and CH_3(e) (red dot Figure 2), is reached at a lower value of the Pauli repulsion than is obtained in the equilibrium geometry of the staggered conformation (green dot). This result does not present a paradox with the finding that the Pauli repulsion is always higher when going to the eclipsed conformation with all other geometry parameters fixed. It only signals the important increase of also the gradient of the Pauli repulsion when going to the eclipsed conformation. This is just one more example of the frequently encountered situation, that the values of the energy terms in the "final" equilibrium geometries may give a misleading picture; the full behavior along the relevant geometry changes has to be considered, see for example, ref. [22].

Let us now turn to the other energy terms, ΔV_{elstat} and ΔE_{oi}. It is interesting to observe that the electrostatic interaction ΔV_{elstat} is slightly more attractive in the eclipsed conformation (red lines below corresponding green lines). The effect is small in this case, but it is generally true that stronger overlap of the charge distributions of the fragments leads not only to higher steric repulsion, but also to a more attractive electrostatic interaction. The attractive nature of the electrostatic term is discussed in refs. [18, 19] In short, the electron–electron repulsion and the nucleus–nucleus repulsion between the two methyl fragments are both large and positive, but the negative electron–nucleus attraction is stronger. It is a general phenomenon (for neutral fragments)[18] that when we let two fragment charge distributions interpenetrate, the total electrostatic interaction is attractive since the electron–nucleus attraction outweighs the repulsive terms. This phenomenon first of all explains the more negative ΔV_{elstat} with shortening C–C separation. Furthermore, when one rotates to the eclipsed conformation with a fixed geometry CH_3, all the terms in ΔV_{elstat} become larger in an absolute sense, but the attractive one slightly more so, hence the more attractive electrostatic interaction for the eclipsed conformation. Similarly, when one bends CH_3 from CH_3(e) to CH_3(s), at a given C–C separation and a given rotation angle, the stronger interpenetration of charges for CH_3(s) than for CH_3(e) leads to more attractive ΔV_{elstat} (solid lines below broken lines in Figure 2). These observations underline the quite general fact that the origin of steric repulsion is not electrostatic repulsion between electron charge clouds and nuclei, on the contrary, the electrostatic term favors steric crowding! It is the quantum mechanical Pauli exclusion principle (which leads to a rise in kinetic energy) that is at the origin of the steric repulsion.

The ΔE_{oi} energy of approximately 180 kcal mol^{-1} largely consists of the electron-pair bonding energy of the C–C σ bond, which we find to be invariant under rotation to at least 0.01 kcal mol^{-1}. There are small additional contributions from the admixing of virtual fragment orbitals (notably σ* C-H) to the orbital interaction term ΔE_{oi}. This term is usually also more attractive when the overlap of the charge clouds is larger, since then not only the occupied–occupied orbital overlaps are larger, but the occupied–unoccupied orbital overlaps are also larger, which leads to stronger donor–acceptor interactions. Remarkably, in this case we find this situation reversed: the orbital interaction is more favorable in the case of the staggered conformation. The preference of about 0.4 kcal mol^{-1} for the staggered conformation arises from the unoccupied/occupied orbital mixing and must be due to the more favorable vicinal σ–σ* overlap in the staggered conformation that has been stressed by Weinhold and others.[1–6] However, we do not find this effect to be quantitatively very important, it is only 0.4 kcal mol^{-1} and it is almost canceled by the approximately 0.3 kcal mol^{-1} preference of ΔV_{elstat} for the eclipsed conformation. The Pauli repulsion clearly stands out as the energy component that discriminates between eclipsed and staggered conforma-

tions, both because of the relatively large difference it makes for the two conformations at all C–C separations, and because of its steeper gradient for eclipsed ethane at shorter separations.

We conclude that our results are in full agreement with the textbook explanation for the preference for the staggered conformation as being due to steric hindrance. At all C–C separations in the range of interest, and for both CH_3(s) and CH_3(e), the steric repulsion is larger for eclipsed ethane. In fact, the steric repulsion is not only weaker in the staggered conformation at each C–C separation and CH_3 conformation, it also increases less steeply with shortening C–C separation and decreasing ∢C-C-H angle (softer repulsive wall). The equilibrium C–C separation therefore becomes shorter in the staggered case, and the ∢C-C-H angle smaller, with the result (only seemingly paradoxical) that an equilibrium geometry is attained where the steric repulsion has reached a higher value than it has at the equilibrium geometry of eclipsed ethane.

The barrier to rotation has been ascribed to Pauli repulsion between vicinal C–H bonds on the basis of more approximate methods a long time ago, notably by Hoyland,[23] Sovers et al.[24] and by Lowe[25] (see refs. [5,6] for extensive references to earlier work). Why does NBO analysis yield a different picture? This is basically because it does not leave the occupied orbital space of canonical orbitals untouched, but mixes the occupied and virtual spaces when transforming to bond orbitals and antibonding counterparts. (We take a single determinantal wavefunction (Hartree–Fock) as reference, which is the level of theory that has been used mostly in the NBO analyses.) The bond orbitals (and core and lone-pair orbitals) are associated with the bonds (and cores and lone pairs) of the Lewis structure. Owing to the procedure for their construction, the NBOs differ from the localized orbitals that can be obtained from the Hartree–Fock wavefunction by a localization procedure. The localized orbitals are nothing but a unitary transformation of the HF orbitals and leave the electron density and total energy unchanged. In contrast, the NBO determinantal wavefunction containing the strongly occupied NBOs ("Lewis determinant"), even though it approximates the density and HF wavefunction rather closely (to better than 99.7%), still is considerably higher in energy than Hartree–Fock (in the case of ethane some 30–40 kcal mol^{-1} higher,[5] that is, an order of magnitude more than the barrier height). Mixing of the antibonding orbitals (such as the σ^*_{C-H} orbitals in ethane) into the bonding orbitals in the NBO determinant leads to energy lowering (called delocalization energy, E_{deloc}) from the Lewis determinant energy E_{Lewis} to the HF energy E_{HF}. This mixing makes the unoccupied (in the Lewis determinant) σ* orbitals weakly occupied, and the bonding orbitals no longer fully (but still strongly) occupied. So the NBO scheme introduces a reference state (the Lewis determinant) which is destabilized compared to the Hartree–Fock determinant, and puts considerable emphasis on the σ* orbitals of the model, as is evident from the energy lowering coming from their admixing. In the present case we note, from the detailed analysis by Goodman et al.,[15] that when we perform a rigid rotation of staggered ethane to eclipsed ethane, keeping the C–C separation and the CH_3 conformation fixed, the energy E_{Lewis} of the Lewis determinant becomes more favorable by 2.68 kcal mol^{-1} (step I in table III of ref. [15]). We would expect at least some steric hindrance effect, and it is unfortunate that a wavefunction that is supposed to correspond to the Lewis structure, does not exhibit the expected steric repulsion between electron pairs when rotating towards a more sterically crowded conformation. This situation would put into jeopardy the very concept of steric hindrance. Of course, when the admixing of the σ* orbitals is allowed in the next step (E_{deloc}), the HF energy and therefore the barrier that is known to exist at the HF level, will be restored. So one can calculate that E_{deloc}, which is large (ca. 35 kcal mol^{-1}), will provide 5.52 kcal mol^{-1} more energy lowering in the staggered conformation. Conversely, when leaving this σ* admixing out, the eclipsed conformation will be preferred.[1] This leads to the contention that it is hyperconjugation and not steric repulsion that causes the barrier in ethane.

Our analysis scheme on the contrary identifies steric repulsion as the cause of the barrier. We prefer this analysis method for the following reasons. It uses the canonical orbitals of the two CH_3 fragments. This has the advantage that these orbitals are unambiguously defined (within the model used, Hartree–Fock for instance, or Kohn–Sham). They diagonalize the fragment one-electron Hamiltonian, that is, they have meaningful orbital energies and there are no zeroth-order couplings between the unoccupied (e.g. σ*) orbitals and the occupied orbitals on the same fragment. The stronger Pauli repulsion we find in the eclipsed conformation fits in with expectations from the steric crowding in that conformation. The behavior of the terms ΔE_{Pauli}, ΔV_{elstat} and ΔE_{oi} is physically completely understandable and is as expected (the trends and observations seen here recur in many applications[19]). The relative unimportance of the σ* orbitals that we find, fits in with the known high energy of these (canonical) orbitals in the CH_3 fragments. Weinhold and co-workers[26] have criticized the use of a virtual orbital space orthogonal to the occupied fragment orbital space, as used by Morokuma[12] to obtain charge-transfer and polarization energies and which we use to obtain the ΔE_{oi} term. It is indeed true that when we allow the bond orbitals in a localized orbital representation of the Hartree–Fock wavefunction to distort slightly to a Lewis structure NBO wavefunction, at the cost of a rise in energy of E_{Lewis} with respect to E_{HF}, the NBO antibonding orbitals, even if orthogonal to the occupied NBOs, can "occupy" some of the space of the occupied canonical orbitals (i.e. the Hartree–Fock orbitals; the equivalent localized orbitals span the same space). So they will without doubt become more "chemically active". However, this raises the issue of the right balance. In particular, when the Lewis determinant shows a reversed steric repulsion effect (i.e. attraction) for the more sterically crowded situation, this begs the question whether the generation procedure for the NBOs has struck the right balance between the "steric" (in E_{Lewis}) and "orbital interaction" or "hyperconjugation" (in E_{deloc}) components of the energy.

Since the concepts we are dealing with in these electronic structure analyses (steric repulsion, bond orbitals, hyperconjugation) are not observables, and not even sharply defined in terms of wavefunctions, we cannot conceive of a

definitive experimental test to decide which model is "right" and which is "wrong". That hyperconjugation is the cause of the barrier in ethane is "true" within the NBO method of electronic-structure analysis. Steric repulsion is the "true" cause in our analysis. When deciding between electronic-structure analysis schemes, one weighs virtues, such as simplicity, physical transparency, lack of arbitrariness. The analysis should also preferably conform to intuitive chemical notions, and should serve the purpose of quantifying and sharpening those. If the electronic-structure analysis method identifies one of its quantities with an intuitive chemical concept, and subsequently finds the quantitative results to be in conflict with accepted notions, one has to face the question whether this quantity in the theory is rightfully identified with the chemical concept, and whether a different quantity from quantum chemical theory might correspond more closely to the concept. Apparently, the use of occupied canonical fragment orbitals to define the steric repulsion is not only simple and unambiguous, it also conforms in this case, as it unfailingly does,[19] to the notion of increasing steric repulsion with more steric crowding. The Lewis structure wavefunction of the NBO analysis in the case of ethane does not do so.

In conclusion, our analysis, which has been applied in many different situations, in the present case fully corroborates the intuitive expectation of steric repulsion as driving force for the barrier in ethane. These results confirm the association of the term ΔE_{Pauli} of Equation (1) with the Pauli repulsion to be meaningful. We conclude that there is no compelling reason for the chemical community to abandon the explanation of the barrier in ethane as arising from steric repulsion.

Received: January 15, 2003 [Z50947]

Keywords: conformation analysis · electronic structure · ethane · rotation barrier · steric hindrance

[1] V. Pophristic, L. Goodman, *Nature* **2001**, *411*, 565.
[2] F. Weinhold, *Nature* **2001**, *411*, 539.
[3] T. K. Brunck, F. Weinhold, *J. Am. Chem. Soc.* **1979**, *101*, 1700.
[4] G. T. Corcoran, F. Weinhold, *J. Chem. Phys.* **1980**, *72*, 2866.
[5] A. E. Reed, F. Weinhold, *Isr. J. Chem.* **1991**, *31*, 277.
[6] J. K. Badenhoop, F. Weinhold, *Int. J. Quantum Chem.* **1999**, *72*, 269.
[7] S. Borman, *Chem. Eng. News* **2001**, *79(50)*, 53.
[8] C. Henry, *Chem. Eng. News* **2001**, *79(23)*, 10.
[9] P. R. Schreiner, *Angew. Chem.* **2002**, *114*, 3729; Angew. *Chem. Int. Ed.* **2002**, *41*, 3579.
[10] K. J. Morokuma, *J. Chem. Phys.* **1971**, *55*, 1236.
[11] K. Kitaura, K. Morokuma, *Int. J. Quantum Chem.* **1976**, *10*, 325.
[12] K. Morokuma, *Acc. Chem. Res.* **1977**, *10*, 294.
[13] K. Morokuma, H. Umeyama, *Chem. Phys. Lett.* **1977**, *49*, 333.
[14] W. England, M. S. Gordon, *J. Am. Chem. Soc.* **1971**, *93*, 4649.
[15] L. Goodman, H. Gu, V. Pophristic, *J. Chem. Phys.* **1999**, *110*, 4269.
[16] T. Ziegler, A. Rauk, *Inorg. Chem.* **1979**, *18*, 1558.
[17] T. Ziegler, A. Rauk, *Inorg. Chem.* **1979**, *18*, 1755.
[18] "Cluster Models for Surface and Bulk Phenomena": E. J. Baerends, *NATO ASI Ser. Ser. B* **1992**, 189.
[19] F. M. Bickelhaupt, E. J. Baerends in *Reviews in Computational Chemistry, Vol. 15* (Eds.: K. B. Lipkowitz, D. R. Boyd), Wiley, New York, **2000**.
[20] F. M. Bickelhaupt, N. M. M. Nibbering, E. M. van Wezenbeek, E. J. Baerends, *J. Phys. Chem.* **1992**, *96*, 4864.
[21] J. D. Kemp, K. S. Pitzer, *J. Chem. Phys.* **1936**, *4*, 749.
[22] F. M. Bickelhaupt, R. L. DeKock, E. J. Baerends, *J. Am. Chem. Soc.* **2002**, *124*, 1500.
[23] J. R. Hoyland, *J. Am. Chem. Soc.* **1968**, *90*, 2227.
[24] O. J. Sovers, C. W. Kern, R. M. Pitzer, M. Karplus, *J. Chem. Phys.* **1968**, *49*, 2592.
[25] J. P. Lowe, *J. Am. Chem. Soc.* **1970**, *92*, 3799.
[26] A. E. Reed, L. A. Curtiss, F. Weinhold, *Chem. Rev.* **1988**, *88*, 899.

